# Novel heart valve leaflet designs with stiff polymeric materials and biomimetic kinematics

Caroline C. Smid[*1], Georgios A. Pappas[1a], Nikola Cesarovic[2,3], Volkmar Falk[2,3,4], Paolo Ermanni[1]

[1] *Laboratory of Composite Materials and Adaptive Structures, ETH Zurich*
[2] *Translational Cardiovascular Technologies, ETH Zürich*
[3] *Klinik für Herz-, Thorax- und Gefäßchirurgie*
[4] *Deutsches Herzzentrum Berlin, Klinik für Kardiovaskuläre Chirurgie, Charité Universitätsmedizin Berlin*

## Graphical abstract

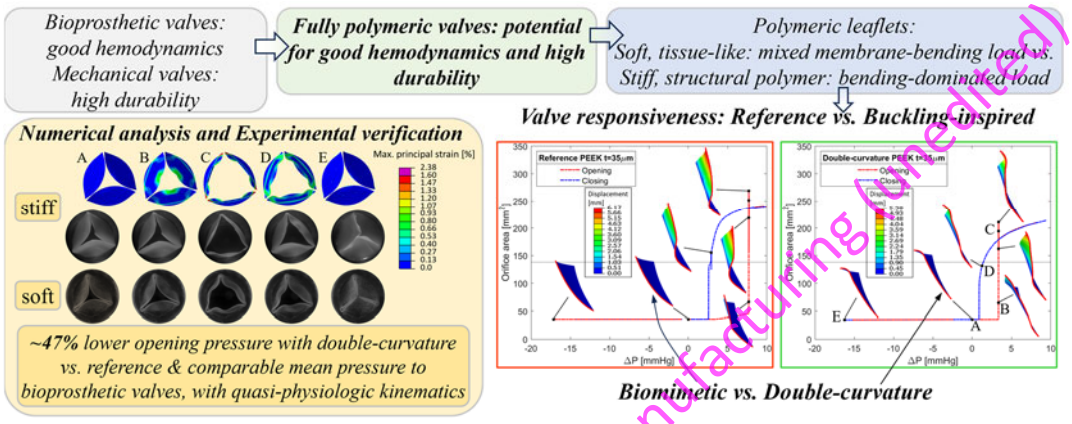


Preprint of Bio-Design and Manufacturing (Unedited)

## Abstract

Despite continuous efforts to improve robustness of cardiac valve implants, neither bioprosthetic, nor mechanical valves fulfill both hemodynamic and durability requirements. This study presents novel flexible leaflet designs, focusing on polymeric materials with proven hemocompatibility, such as PEEK, of much higher stiffness than native tissue, aiming on optimal valve implants. A biomimetic valve with a single-curvature belly-curve serves as reference for the new design variants with a double-curvature belly-curve with varying radii. Soft (13.2 MPa), as well as stiff (2.4 GPa) leaflet materials, and different thicknesses are studied by means of lean simulations, and in-vitro experiments under physiologic hemodynamic conditions. The performance is assessed by opening pressure and orifice area. The latter is determined by a newly developed automatized image processing tool. Experimental trends are in agreement with simulations and demonstrate that a buckling inspired, double-curvature leaflet design, significantly enhances tri-leaflet valves' opening behavior, particularly advantageous for stiffer leaflet materials. Best performing variant shows an opening pressure improvement in the range of 47% and 44% based on simulations and experiments, respectively, compared to reference, while achieved mean pressure differential is directly comparable to state-of-art bioprosthetic valves. The orifice area is slightly reduced for new variants, yet still in satisfying range.

[*]Corresponding author: csmid@ethz.ch (C. Smid), ETHZ, Leonhardstrasse 21, 8092 Zürich, Switzerland
[a] CS & GP equal contribution

**ORCiD:** CCS: 0009-0008-2440-1892; GAP: 0000-0003-1570-6885; NC: 0000-0001-6744-2928; VF: 0000-0002-7911-8620; PE: 0000-0003-0158-3845

**Keywords:** fully polymeric heart valve; parametric leaflet design; Finite Element Analysis; leaflet kinematics; in vitro testing;

## Article Highlights

- Novel polymeric heart valve designs with moduli 2 – 3 orders higher than native tissue for balanced responsiveness & durability
- Lean simulations & in vitro test confirm efficiency; Best, buckling-inspired design has ~50% lower opening pressure than biomimetic valve
- Design accommodates flexible PEEK leaflets with quasi-physiologic kinematics; mean pressure matches bioprosthetic valve

Preprint of Bio-Design and Manufacturing (unedited)

## 1. Introduction

Two types of contemporary heart valves exist. Mechanical bileaflet valves made from carbon (or titanium) provide long-term durability, but also poor hemodynamics that can lead to flow cavitation [1] and therefore need life-long anticoagulation. Bioprosthetic heart valves (BHVs), on the contrary, consist of leaflets made from bovine or porcine pericardium mounted on a fixed (surgical implants) or expandable (transcatheter valves) stent frame, after a labor intense process. While long-term anticoagulation is not required with BHVs, they are subject to leaflet degeneration, which typically results in structural valve failure during longer term follow-up, and limits their durability. The life-time management for treating valvular heart disease, therefore includes, implant related factors such as the need for anticoagulation and durability, as well as patient related factors, such as age at time-of-index operation, comorbidities, access, and patient preferences. [2]

With the demographic change, the increasing demand for heart valves is expected to surpass 850,000 annually worldwide by 2050. [3] Given the current limitations of state-of-the-art valve technology, it is crucial to explore new valve concepts that provide improved durability without compromising the hemodynamic performance. This includes the use of new materials, innovative designs, and advances in manufacturing techniques. To date, no FDA-approved valve has successfully combined the long-term durability, typical of mechanical heart valves (MHVs), without the need of anticoagulation. [4]

Considering the limitations of available materials emulating natural leaflet compliance, such as poor durability, it seems necessary to explore alternative options, including stiffer materials, which could, however, result in poor hydrodynamics. [5] For instance, MHVs made with ~2000× stiffer materials [6], employ a two (or three) flat-disk design, instead of an anatomical design, like the native valves. Fully polymeric heart valves (PHVs) with robust leaflets made from strong and stiff polymeric materials pose a promising solution. These materials can be even ~300× stiffer than natural leaflet tissue [7] in terms of Young's modulus, but also of higher strength. Nevertheless, the utilization of significantly stiffer (and stronger) leaflet materials necessitates a novel valve design to achieve the requested leaflet kinematics at low pressures.

In this study, novel leaflet design concepts that may facilitate the use of stiff materials, are

Preprint of Bio-Design and Manufacturing (unedited)

introduced, and analyzed by lean solid mechanics based finite element (FE) simulations and assessed by in-vitro hydrodynamic experiments, using a custom-built pulse duplicator (PD). [8] The ultimate objective is to incorporate stiff material leaflets, with proven hemocompatibility, such as Polyether ether ketone (PEEK) [9], into a heart valve design able to approach the kinematics and hemodynamic performance of best-in-class BHVs, approaching a native valve. Motivation for use of PEEK is high, as it shows low-thrombogenicity based on an animal trials conducted without antithrombotic medication [10] with a valve featuring rigid PEEK leaflets [11]. While predominantly considered inert, PEEK can also support endothelialization through surface modification [12].

## 2. Background

Valve design performance assessment criteria, across all prosthesis types, include low transvalvular opening pressure (OP), large orifice area (OA), and tight closing. Research on flexible synthetic PHVs started almost simultaneously with durable MHVs and hemocompatible BHVs. Durability refers to valve's ability to withstand long-term operation without significant degradation or structural failure, considering factors such as material aging, calcification, and stress induced wear due to fatigue loading imposed during the cardiac cycle. Hemodynamics refer to flow dynamics and performance characteristics of a heart valve within blood circulation, identified by parameters such as pressure differentials (often referred as pressure gradient [13]) and flow characteristics, assessing flow obstruction or regurgitation. [14]

Polymers offer design freedom and simple manufacturing processes. Yet, despite design variations and materials attested, including polyurethane (PU), polytetrafluoroethylene, and silicone compounds, such PHVs initially showed insufficient biostability and poor durability. [15] Only after a big leap in the field of material science and nanotechnology, PHVs came back into focus [15–17, 14], with new concepts to include segmented copolymers and polymer nanocomposites [18–20]. Despite these advancements, PHVs have not been able to mimic native valve properties.

Native materials typically exhibit a Young's modulus in the range of 0.03 – 90 MPa. [17, 14] Specifically, native aortic leaflet tissue has elastic moduli of ~4 and ~15 MPa in the radial and circumferential direction, respectively [21], attributed to the circumferential orientation of

Preprint of Bio-Design and Manufacturing (unedited)

collagen fibers [22]. Both first, and new generation polymers, generally fall within the moduli range of native materials, with some reaching 200 MPa [17, 14] and 4 – 100 MPa [17, 14], respectively.

Examples of currently examined PHVs from the international community are detailed in Table 1. While making notable advancements, limitations persist and there is still no FDA-approved PHV, with PHVs only commercially available in ventricular assist devices (VAD). [23] Recognizing the essential need for non-invasive implantation and the persisting challenge of ensuring reproducible manufacturing of soft polymeric leaflets [24], a revised approach is being pursued.

**Table 1: Examples of currently investigated PHVs by international community, with key specifications.**

| PHV Model | Material & Design | Key Information |
|---|---|---|
| AorTech valve (RUA Life Sciences) | Elast-Eon (specially developed biostable PU) with stress-reducing design | 1st generation patented by Fisher [25]; durability of 800 million cycles [26] (exceeds min. requirements of BHVs [27, 28]). |
| PoliValve | Styrenic block copolymers with cylindrically shaped leaflets | Surgically implanted; in vitro performance above standard values [13] (expected durability 30 years); feasibility in short-term in vivo trial [29, 30]. |
| Tria by Foldax | "Bio-inspired" design, biopolymer leaflets, PEEK stent, PTFE sewing ring, automated manufacturing [18] | FDA-approved early feasibility studies show promising results; minimal calcification traces in animal trials; one valve passed 670 million cycles (16 years) with minimal damage. [31, 32, 18] |
| Lapeyre-Triflo FURTIVA | Three non-biomimetic stiff PEEK disk-like leaflets [33] | Tri-leaflet valve with early closing characteristics resembling BHV, potentially eliminating long-term anti-coagulation therapy; limited to surgical implantation. [34, 33] |

Preprint of Bio-Design and Manufacturing (unedited)

Preliminary evaluation of heart valve designs has shifted from experiments [35] and animal trials [36], to advanced simulations. Solid mechanics based simulations [37, 28, 38–40] offer efficiency, acknowledging the simplification in boundary conditions [23], while fluid-level simulations mainly focus on hemodynamics [37]. Fluid-structure interaction simulations provide more accurate predictions, albeit at a much higher computational cost [23, 37], thus often adopted at design verification phase. While advanced simulations hold promise for optimizing heart valve prosthesis designs, the results of such simulations depend heavily on modeling approximations. Conventional in vitro and in vivo tests are therefore still vital to provide input for design iterations

and modeling, and mainly validate promising designs. [37]

# 3. Materials and Methods

## 3.1 Leaflet design & conceptualization

### *3.1.1 Design benchmarking*

Understanding the behavior of leaflets is crucial for improving valve design and performance. These leaflets experience complex transitions during opening and closing, with the sagittal leaflet cross-section, namely the belly-curve (B-C), undergoing the most significant shape transformation. Hence, this study emphasizes on design modifications related to the B-C's shape.

The reference valve is a tri-leaflet aortic valve (AV), which has a continuously increasing radius of curvature away from its center. Previously published literature [35, 25] is used to replicate this valve which is based on conventional single-curvature leaflet designs Fig. 1b, approximating native AVs (Fig. 1a). Leat and Fisher [35] altered both geometry and thickness ($t$), intending to enhance valve's OP. They utilized a material approximately one order of magnitude stiffer (at low strains) than natural leaflet tissue, asserting a relationship expressed as OP$\sim\frac{Et^3}{{R_i}^3}$, assuming a clear bending load dominance, where $R_i$ is the radius of curvature, and $E$, material's Young modulus. [35] The comparison between previously used spherical leaflets and reference valve leaflets (Fig. 1c) revealed that the latter exhibit superior OP under steady flow conditions, however, not in pulsatile flow scenarios.

Preprint of Bio-Design and Manufacturing (unedited)

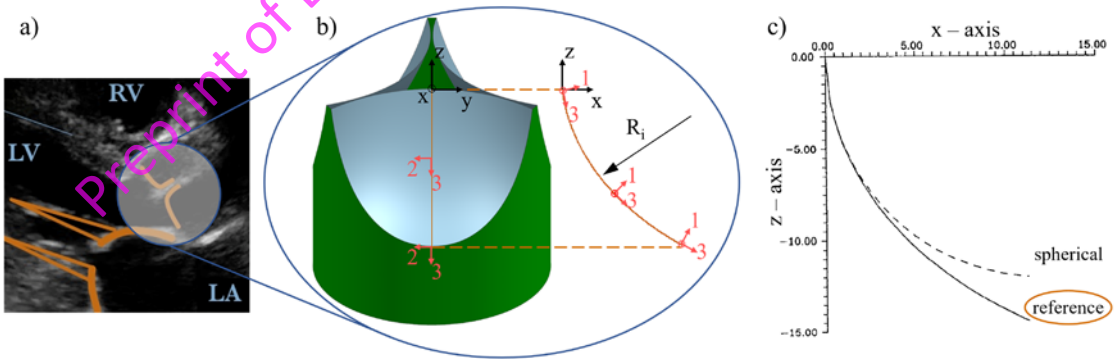


**Fig. 1: a) Echography of a native AV with B-C indicated in orange (reprinted from [41]). b) Rendering of PHV 3D model based on [35, 25]; a mock continuous stent (in green) is also designed for better valve impression; B-C with adopted coordinate system is also shown. c) State-of-the-art B-C geometries (adapted from [35]).**

### *3.1.2 Understanding the mechanics to create a robust design*

Conventional biomimetic leaflets are expected to experience a combination of membrane and bending loads. The bending-dominated part of the response has buckling characteristics, often

enabling rapid responsiveness. Examination of fundamental configurations, including flat, cylindrical & spherical panels, with low thicknesses (Fig. 2a – c) for enhanced deflection under low loads, indicates that flat panels (Fig. 2d) demonstrate the lowest initial stiffness, requiring minimal load for deflection. However, as the applied load increases, the stiffness rises exponentially due to membrane loading, resulting in relatively limited maximum deflection. Conversely, curved panels (Fig. 2d) exhibit decreasing stiffness with load after a certain threshold. [42]. Both cylindrical (Fig. 2b) and spherical (Fig. 2c) panels have a similar high initial stiffness, but can also achieve a high maximum deflection. However, the cylindrical design presents a notable snap-through behavior with secondary stable states (Fig. 2d). [42] Thus, an additional force is needed for recovery, potentially affecting valve closing adversely. Hence, for given boundary conditions, a spherical leaflet shape shows improved deflection characteristics.

In order to further elaborate on the mechanical behavior of biomimetic leaflets, sphere-shaped thin panels are simulated (PEEK material with thickness of 50 µm, see also section 3.3) with radii $R_1 = 10$, 20, and 40 mm (Fig. 2e – g) with a constant base diameter of 10 mm, and subjected to a point load at the middle with hinged edges. The trend shown in Fig. 2g, indicates a decrease in buckling force with an increase in radius, implying that leaflet designs with large $R_1$ might exhibit superior performance in OP. Boundary conditions of valve leaflet have important impact on these results, yet they already provide useful insights.

Designs require adaptation to accommodate materials with stiffness 2 – 3 orders of magnitude higher, compared to natural tissue. To further enhance the deflection tendency, the transitioning from a single-curvature B-C to a double-curvature design (Fig. 2e) is attested. Double-curvature designs resemble an imperfection, which can promote buckling [43], while asymmetric imperfections enhance further the buckling phenomena [44]. Moreover, the double-curvature design offers increased surface area across the same span, enabling greater force component in the opening direction, for a given pressure.

Preprint of Bio-Design and Manufacturing (unedited)

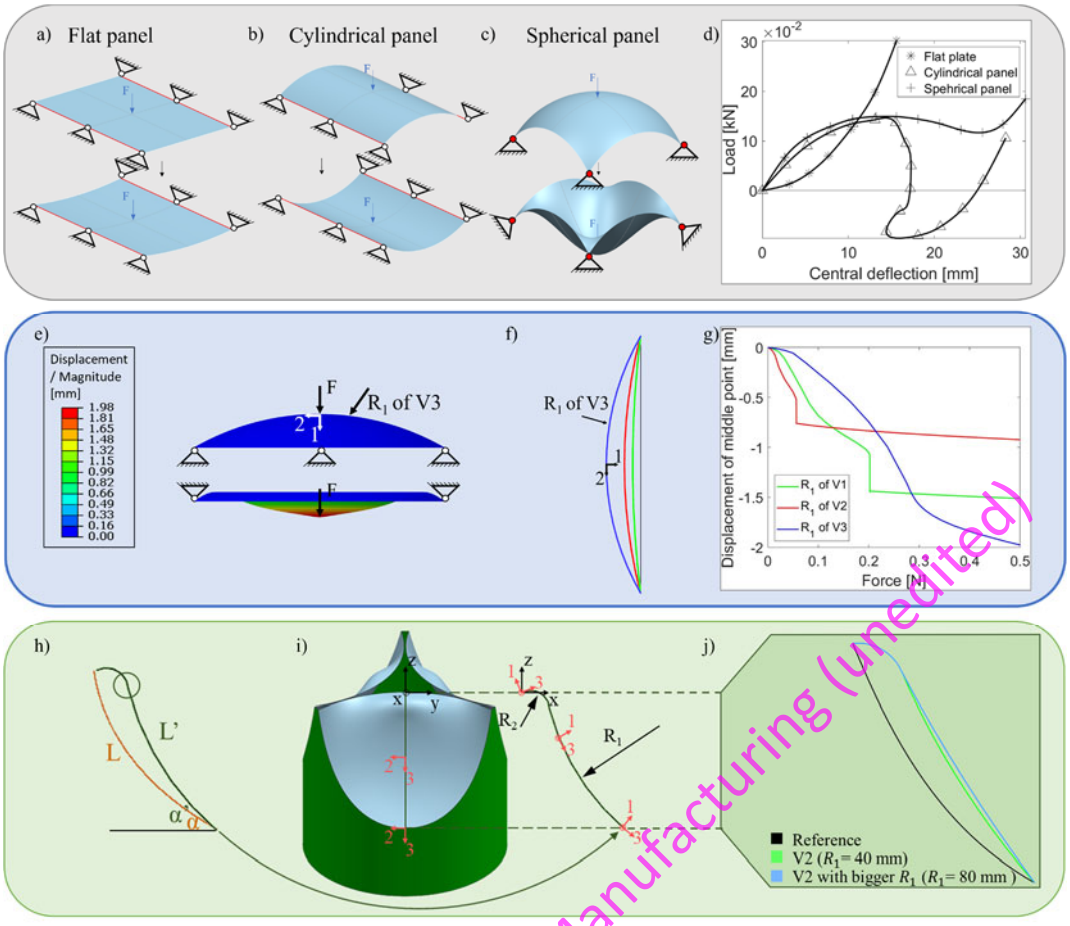


**Fig. 2: a), b) & c) Schematics, not to scale, of basic panel geometries hinged along red edges and corners: flat, cylindrical & spherical. d) Their deflection upon central load (adapted from [42]). e) Simulation of spherical panel with hinged edges and applied point load in the middle, conducted for three different leaflet radii shown in f). g) Displacement of the middle point over the point load. h) Geometrical differences between single- and double-curvature (see also Table 2). i) 3D valve model and its B-C with coordinate system for V5. And j) alternative, potentially more optimal, B-C shape.**

In this study, a B-C with double-curvature was adopted and also studied in a parametric manner, by varying radii $R_1$ and $R_2$ (see Fig. 2i), resulting in 5 variants, as illustrated in Table 2. Valve diameter, shape of OA in the stress-free state, and stent base geometry were kept alike (see also 3.3). Valve's leaflets [35, 25] were designed (NX 12.0, Siemens Industry Software Inc., Texas, USA) in a semi-open position, with an initial OA of ~36 $mm^2$ (stress-free state), with valve inner diameter of 22 mm (nominal OA = 380 $mm^2$). Note that the starting point of $R_2$ coincides with the end point of $R_1$, resulting in a steeper inclination of the B-C due to the geometrical boundary conditions (Fig. 2h).

Preprint of Bio-Design and Manufacturing (unedited)

Table 2: Radii $R_1$ and $R_2$ for each variant in mm and cross-sections of B-C

| | Reference | V1 | V2 | V3 | V4 | V5 |
|---|---|---|---|---|---|---|
| $R_1$ *or* $R_{max}$ *[mm]* | 56 | 20 | 40 | 10 | 20 | 20 |
| $R_2$ *or* $R_{min}$ *[mm]* | 15.3 | 2.3 | 2.3 | 2.3 | 3 | 1.6 |
| | 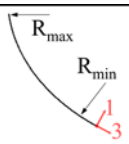 | 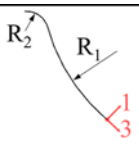 | 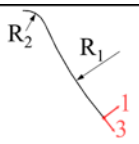 | 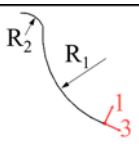 | 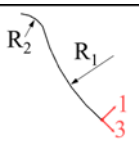 | 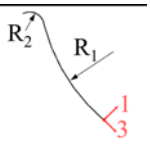 |



### 3.2 Materials

Leaflets made of conventional soft PU (CARBOTHANE™ PC-3585A) are considered for referencing and compared with stiff PEEK foil-based ones. All relevant information is explained hereafter.

### 3.3 Finite Element Analysis

The surface models of the six valves were imported into ABAQUS v6.14 (Dassault Systèmes, France) to conduct a quasi-static, implicit analysis. Shell elements (S4R), with quad-structured mesh, in the range of 20'000 – 24'000 and an 0.2 mm edge, were chosen after an OA-OP response convergence study. Given the potential instabilities (or multi-stabilities) one may have considered to use the Riks method [45, 46]. Nevertheless, given the involved leaflet contacts, a Newton-based solver was chosen [47], while taking care of the increment size, to be sufficiently fine, as this is expected to increase the reliability of the simulations. The increment size was attested by OA-OP response convergence. Only leaflets were modeled, and the stent was approximated as fully rigid by fixed boundary conditions along the leaflet-stent edge (Fig. 3a). A rigid stent is assumed to isolate leaflet geometry's effect, but also neglecting potential stent's flexibility. Hard contact interaction was included to prevent inter-leaflet penetration, assuming a shear friction coefficient of 0.3 [38] & 0.4 [48] for PU and PEEK, respectively. Additionally, a symmetry boundary condition along B-C (Fig. 3a) prevented leaflet twist that related to master-slave surface contact definition in-between adjacent leaflets.

With the opening in focus, a uniformly distributed pressure was applied on the ventricular surface of the leaflet, imposing a linear increase up to the indicative 50 mmHg, to model the pressure differential ($\Delta P$). While the experimental $\Delta P$ of the investigated valves never exceeded

Preprint of Bio-Design and Manufacturing (unedited)

33 mmHg, 50 mmHg was employed in the numerical analysis to ensure valve opening, especially for thicker, and consequently stiffer leaflets. Furthermore, to capture the full kinematic behavior (i.e., valves' opening and closing), a pressure history of [0, 10, 0, -20, 0] mmHg (i.e., one cycle: systole, diastole) was applied, while the boundary conditions stayed the same. Note that the OP for this last assay corresponds to a high level of physiologic pressure. [49, 50] In a previous study by Smid et al. [8], this range was also confirmed for a BHV, with pressure increasing from ~0 – 10 mmHg during leaflet separation to full opening (see Supplementary Material, -SM-, Appendix A).

PU and PEEK were modelled as linear elastic materials with a Young's modulus, $E$, of 13.2 & 2400 MPa (expected between 1900 – 3300 MPa depending on crystallinity [9, 51]) and a Poisson's ratio of 0.48 [52, 53] & 0.4 [54], respectively. PU's tensile strain at break reaches 450% [55], indicating its hyperplastic behavior. Nevertheless, PU was still modeled as an elastic material as recorded strains were below 12%, rendering hyperplastic modeling redundant. The Young's modulus was evaluated based on the reported shore hardness. [56, 57] Leaflet thicknesses, $t$, of 150 [35] & 300 μm were investigated for PU. According to the first-order approximation by Leat and Fisher [35] PEEK leaflets, i.e. OP$\sim Et^3$ (for given curvature), for PU leaflets with $t = 150$ μm PEEK, should have a thickness of $t = 26.5$ μm; this value was considered along with 35, 50, and 75 μm.

In order to assess the load state details, the bending and membrane strain energy ratio was calculated for soft and stiff material leaflets, for the most promising design at opening (①) and maximum pressure (②) instants (Fig. 3d). Instant ② was selected near the experimental maximum $\Delta P$ of PEEK leaflets. Element volume was extracted for the two element rows along B-C, as well as stress components, $\sigma_{22}$ and $\sigma_{33}$, as a function of shell thickness (bottom: $-\frac{t}{2}$, top: $\frac{t}{2}$). The membrane stresses ($\sigma_{ii}^m$) were then computed based on the superposition principle (Fig. 3b) as follows:

$$\sigma_{ii}^m = \frac{(\sigma_{ii})_{top} + (\sigma_{ii})_{bottom}}{2} \quad (1)$$

The bending slope, and consequently the curvature, $\kappa_{ii}$, were calculated as follows:

Preprint of Bio-Design and Manufacturing (unedited)

$$\kappa_{ii} \cdot E = \frac{(\sigma_{ii})_{top} - (\sigma_{ii})_{bottom}}{t} \tag{2}$$

Next, the bending strain energy ($U_b$) can be calculated as follows:

$$U_b = \int_V \frac{1}{2}\sigma\varepsilon dV = \int_{-\frac{t}{2}}^{\frac{t}{2}} \frac{1}{2}\frac{\sigma^2}{E} A dy = \int_{-\frac{t}{2}}^{\frac{t}{2}} \frac{1}{2}\frac{(\kappa E t)^2}{E} A dy = \frac{1}{2}\frac{\kappa^2 E t^3}{12} A \tag{3}$$

with $\varepsilon$ and $A$ being the strain and cross-sectional area, respectively. The membrane strain energy ($U_m$), based on the membrane stress, is calculated in a similar manner:

$$U_m = \int_{-\frac{t}{2}}^{\frac{t}{2}} \frac{1}{2}\frac{(\sigma_{ii}^m)^2}{E} A dt = \frac{1}{2}\frac{(\sigma_{ii}^m)^2}{E} A \tag{4}$$

The bending strain energy ratio ($\psi$) over the total strain energy, along B-C, is defined as:

$$\psi = \frac{U_b}{U_b + U_m} \tag{5}$$

Preprint of Bio-Design and Manufacturing (unedited)

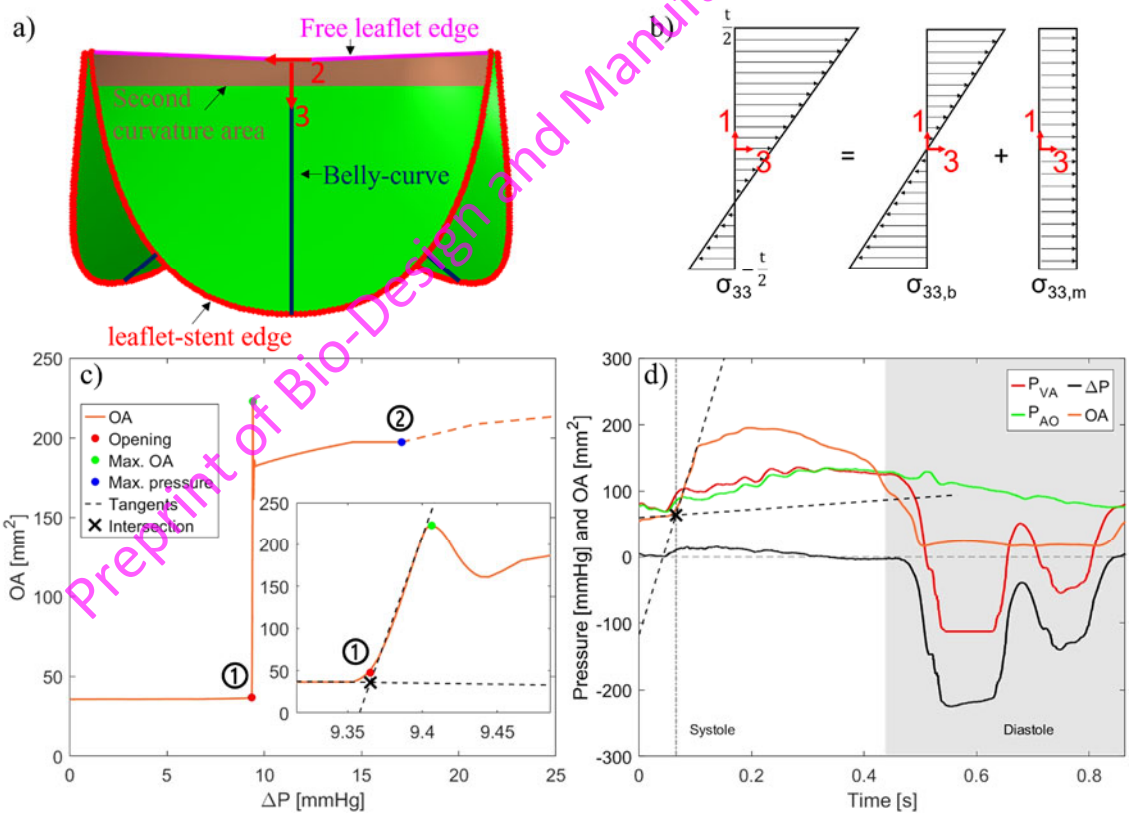


**Fig. 3: a) Leaflets with their boundary conditions and directions 2 and 3. b) Schematic of superposition principal for stress/strain calculation. c) Numerical OA over $\Delta P$ of V2 (PEEK, $t$ = 50 µm) with tangents to determine the opening point -①-, maximum OA, and maximum pressure -②-. d) Experimental pressures and OA of V2 (PEEK, $t$ = 50 µm) with opening point.**

To calculate the geometrical OA, the nodal coordinates from every increment are loaded into an in-house built MATLAB script. The script creates a bounding area from the coordinates for

each step, plotting the projected OA over $\Delta P$. The opening point is then defined as the intersection between flat closed part (as pressure builds-up) and the steep opening phase (Fig. 3c, d). The maximum OA is evaluated right after valve's opening (typical curve shown in Fig. 3c), as pressure continuous to build-up, without any meaningful flow equivalent given the quasi-static simulation. Under typical physiologic flow conditions, a $\Delta P$ drop after valve's full opening is expected (as also shown Fig. 3d).

### 3.4 Experimental assessment

#### *3.4.1 Valve fabrication*

For the PU leaflet manufacturing, a 3D-printed, polymer mold (Therma 280, DWS) with a mounted stent of equivalent material, was dip-coated into a 20% (w/v) PU solution in N,N-dimethylacetamide (DMAc), targeting a thickness of 150 µm. [25] PEEK leaflets were manufactured by vacuum forming a PEEK foil (Victrex APTIV® 2000, Lancashire, UK) using the equipment presented in [51], onto an aluminum mold with alike 3D-printed stents, with the foil subsequently being glued (Scotch-Weld-2216-B/A-Grey) to the stent (Fig. 4). At very low leaflet thickness, the material becomes fragile, particularly under membrane loads during manipulation (in view of implantation). Successful valve prototypes were produced with a 50 µm PEEK foil, highlighting the importance of a responsive valve design at this thickness despite the evident rise in bending stiffness. It is important to note that the membrane's load limit is directly proportional to the leaflet thickness.

The aforementioned PHVs were also compared with a BHV (Edwards INTUITY inner diameter: 21 mm, Edwards Lifesciences, Irvine, CA) and MHV (Medtronic Advantage outer diameter: 27 mm and ID: 23 mm).

#### *3.4.2 Pulse duplicator set-up*

The experiments are performed with a PD as described in Smid et al. [8] (Fig. 4). A brief mention is made here for completeness. The AV models are placed in a compliant 3D-printed (Elastic 50A Resin, Formlabs, MA, USA) aortic root model [58] between the outlet of the pulsatile pump (ViVitro Systems Inc., Victoria, Canada) (representing the left ventricle) and a compliance chamber (mimicking aortic and systemic compliance). Pump's inlet and reservoir (representing the left atrium) are separated by a BHV (Edwards INTUITY 21 mm, Edwards Lifesciences, Irvine,

Preprint of Bio-Design and Manufacturing (unedited)

CA) acting as mitral valve. Distilled water circulates at room temperature (21 ± 2°C). The pulsatile pump creates sinusoidal flow with adjustable amplitude and frequency, maintaining a systole/diastole ratio of $^1/_2$. The piston position ($\Delta(t)$) defines the imposed volume rate ($\dot{V}$) and heartbeat.

Valve behavior evaluation encompasses flow measurements, high-fidelity pressure data, and real-time imaging using a high-speed camera. All these acquired data are analyzed using an in-house MATLAB script, with device output signals recorded by a microcontroller board equipped with a 12-bit analog to digital converter, ADC, (Arduino Due). The aortic flow rate ($Q_{AV}$) upstream of the AV, is measured with a flow sensor (SONOTEC GmbH, Halle (Saale), Germany), accuracy of ± 100 ml/min for 0 – 5 l/min). The actual cardiac output (CO, l/min), as well as the regurgitation are determined based on instant $Q_{AV}$ data.

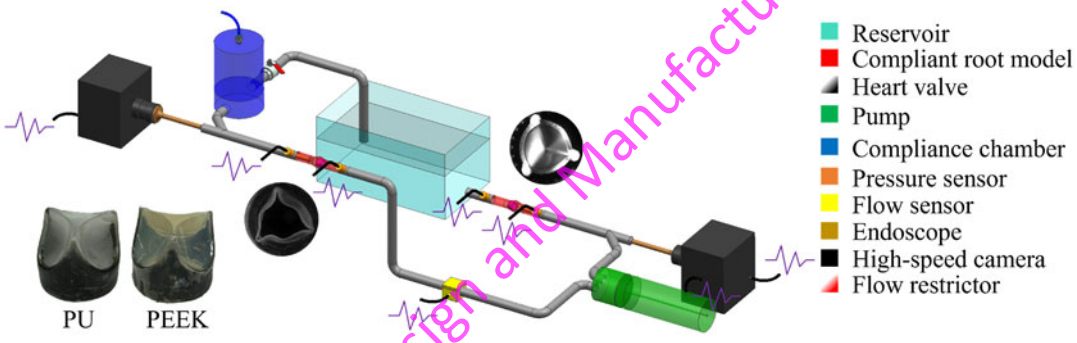


**Fig. 4: Schematic of PD (see also [8]) and investigated PU & PEEK valves.**

Two hydrostatic pressure sensors (Sensata Technologies, Attleboro, MA, United States) are positioned about 80 mm upstream and downstream of the AV measuring the ventricular-aortic ($P_{VA}$) and aortic ($P_{AO}$) pressure, respectively. Pressure is measured in a range of 0 – 375 mmHg (zero reference in atmosphere) with a fidelity (linearity and hysteresis) of at least 0.025% of the full range, matching the ADC-system resolution of 0.9 mmHg. $\Delta P(t)$ is evaluated over a full cycle and is calculated as:

$$\Delta P(t) = P_{VA}\,(t) - P_{AO}\,(t) \tag{6}$$

The mean pressure differential ($\Delta\bar{P}$) is the average $\Delta P(t)$ per cycle, keeping only positive values. [13]

A laparoscopic endoscope (Hopkins II, Karl Storz, Tuttlingen, Germany) is inserted

Preprint of Bio-Design and Manufacturing (unedited)

downstream into a 45°-Y-fitting, laying coaxial to the AV and valve's motion is recorded with a high-speed camera (FASTCAM Mini UX100, Photron USA Inc., San Diego, CA and MeVis-C 1.6/35 macro lens, LINOS, Göttingen, Germany), positioned directly on the endoscope, at 250 fps and 1280×1024 pix$^2$ resolution. A light source illuminates the heart valve. Trigger and image-capture events are fed to the ADC (fidelity of 125 µs) for synchronized data acquisition. Concurrently, pressure, flow, and piston-position data are recorded with a sampling rate of ~3 kHz. Final reported values are averaged over ten consecutive cycles. Each valve was evaluated under normotensive pressure hemodynamic conditions (120/80 mmHg), at a heart rate of 70 bpm, and CO of 5 l/min following ISO5840-3. [13] The compliance chamber and flow restrictor were adjusted accordingly.

### *3.4.3 Orifice area tracking*

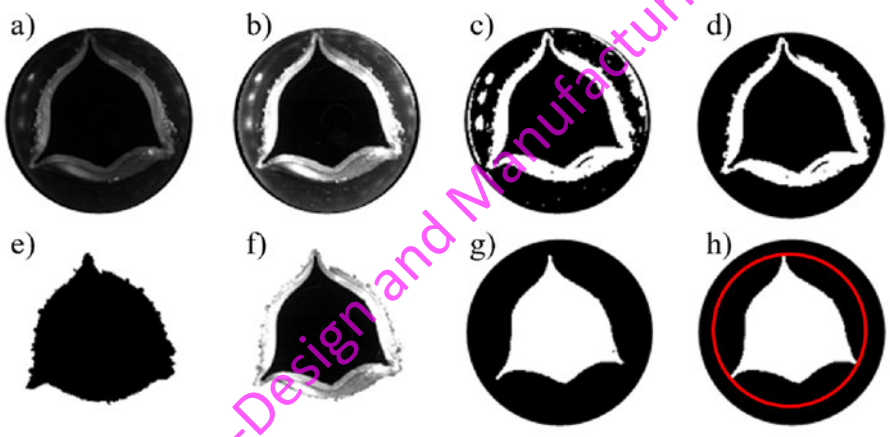


**Fig. 5: OA tracking steps: a) initial image-gray scale (8 bit); b) image with enhanced contrast; c) binarized image b); d) largest object isolation; e) created mask from image d); f) cropped image b) with mask; g) largest binarized object in f); h) final image with artifacts corrected (see text for details). The red circle indicates valves' cylindrical stent base.**

Preprint of Bio-Design and Manufacturing (unedited)

Recently, researchers [33, 59] have applied some effort to track the OA using optical/pure imaging techniques. Nevertheless, given the objective of this study on evaluating alternative valve concepts, a more versatile and valve invariant technique had to be developed in a MATLAB 2022a environment, leading to an automatized image processing tool. The process' intermediate results are depicted in Fig. 5. Firstly, contrast is enhanced to highlight leaflet domains for subsequent binarization. (Fig. 5b). Then, valve leaflet roots are tracked (Fig. 5c, d) and used as a mask to isolate the outer dark area (Fig. 5e). This leads to a distinct tracking of the OA (in black in Fig. 5f). Finally, artifacts, like air bubbles are suppressed (Fig. 5g, h), and pixel sum is calculated. To correlate pixel-size in mm, a white reference circle of known diameter is positioned and imaged

up-front the heart valve before staring any trial.

# 4. Results and Discussion

## 4.1 Numerical analysis

PU and PEEK leaflets were simulated for alike flexural stiffness $Et^3$, in order to assess the validity of the first-order approximation (OP~$Et^3$) by Leat and Fisher. [35] The results presented in Fig. 6a do not support this initial hypothesis. The OPs for PEEK leaflets were up to 2.5× higher than PU. This suggests that bending-dominated load assumption is weak and insufficient for design scaling as further demonstrated in Fig. 6b, where PU ($t$ =150 & 300 µm, solid lines) and PEEK ($t$ = 26.5, 35, 50 & 75 µm, dashed lines) do not follow the same path. Generally, PU has lower OPs than PEEK, attributed to the neglected membrane contribution, as explained in section 0.

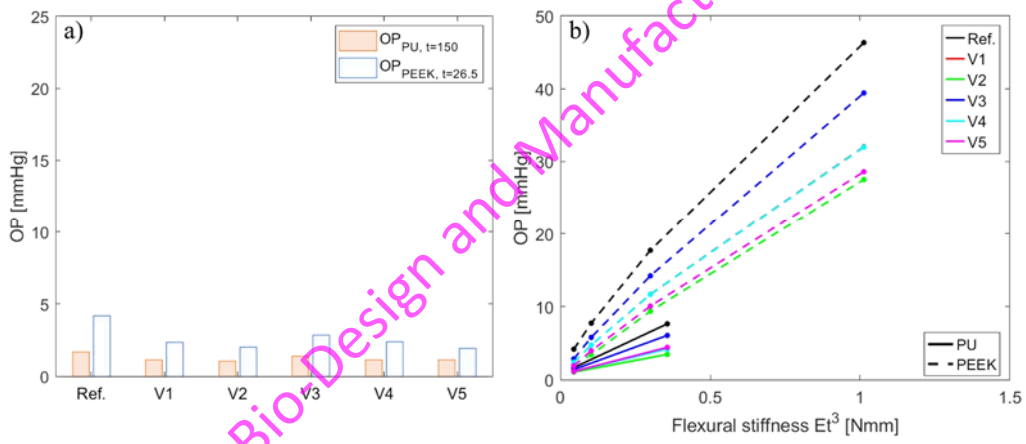


**Fig. 6: OP for designs considered a) for constant $Et^3$ for PU ($t$ = 150 µm) and PEEK ($t$ = 26.5 µm) and b) for varying $Et^3$ for PU ($t$ = 150 and 300 µm) (solid line) and PEEK ($t$ = 26.5, 35, 50, and 75 µm) (dashed line). Note the difference in OP scale.**

### *4.1.1 Valve designs*

The numerical analysis highlights a distinct trend in valve responsiveness summarized in section 4.2. Generally, the new designs exhibited significantly lower OPs compared to the reference, especially with stiff leaflet materials. V2 stands out with the lowest OP, measuring 1.1 mmHg and 9.4 mmHg for PU ($t$ = 150 µm) and PEEK ($t$ = 50 µm), respectively. This design provides the most significant improvement for PEEK, $t$ = 35 µm, where OP is reduced by 56% compared to the reference, with the equivalent for $t$ = 50 µm to be 47%. PU – based comparison still shows equivalent improvement with 37% for $t$ = 150 µm, and 55% for $t$ = 300 µm, with

Preprint of Bio-Design and Manufacturing (unedited)

thicker leaflet to benefit more for this case. In contrast, V3 shows the lowest responsiveness, with an OP ~20% lower compared to the reference for PEEK ($t = 50$ μm). The numerical $\Delta P$ – OA paths of depictive variants can be found in the SM (Appendix A).

Overall, these results suggest that the double-curvature leads to a higher leaflet responsiveness, based on OP, attributed to a reduced effective flexural stiffness. A large $R_1$ and a small $R_2$ favor lower OP. It appears that $R_1$ has a greater influence on reducing OP, as evidenced by the superior performance of V2 with a larger $R_1$ compared to V5 with a smaller $R_2$. Furthermore, the influence of $R_2$ on the OP becomes significant only below a certain value, as indicated by the similar performance of V1 and V4. A slight reduction in OA for the new designs is noticeable, although all exceeded the range of 138 $mm^2$, reported in the norm [13], for the given nominal diameter (i.e. 22 mm). V5 had the smallest OA, up-to 26% smaller compared to the reference design. This discrepancy may be attributed to the smallest $R_2$ of V5 limiting its ability to open as widely, as illustrated in the SM.

#### *4.1.2 Opening and closing behavior*

Fig. 7 illustrates noticeable differences in the trajectories of opening and closing OA for the reference design and V2, for both soft and stiff leaflet materials (see SM, Appendix B, for other variants). The abrupt leaflet response relates to instabilities seen through the snap-through of the shell structure. During valve opening and closing, a change in leaflet curvature is occurring, a phenomenon previously reported by other researchers and common in aortic leaflets. [60] An 'apparent hysteresis' is observed, namely closing occurring at lower pressures than opening. PU leaflets tend to stretch more under high pressures, while PEEK leaflets exhibit more diverse curvature patterns driven by bending instabilities (see provided video), which apparently led to states with higher stiffness.

Preprint of Bio-Design and Manufacturing (unedited)

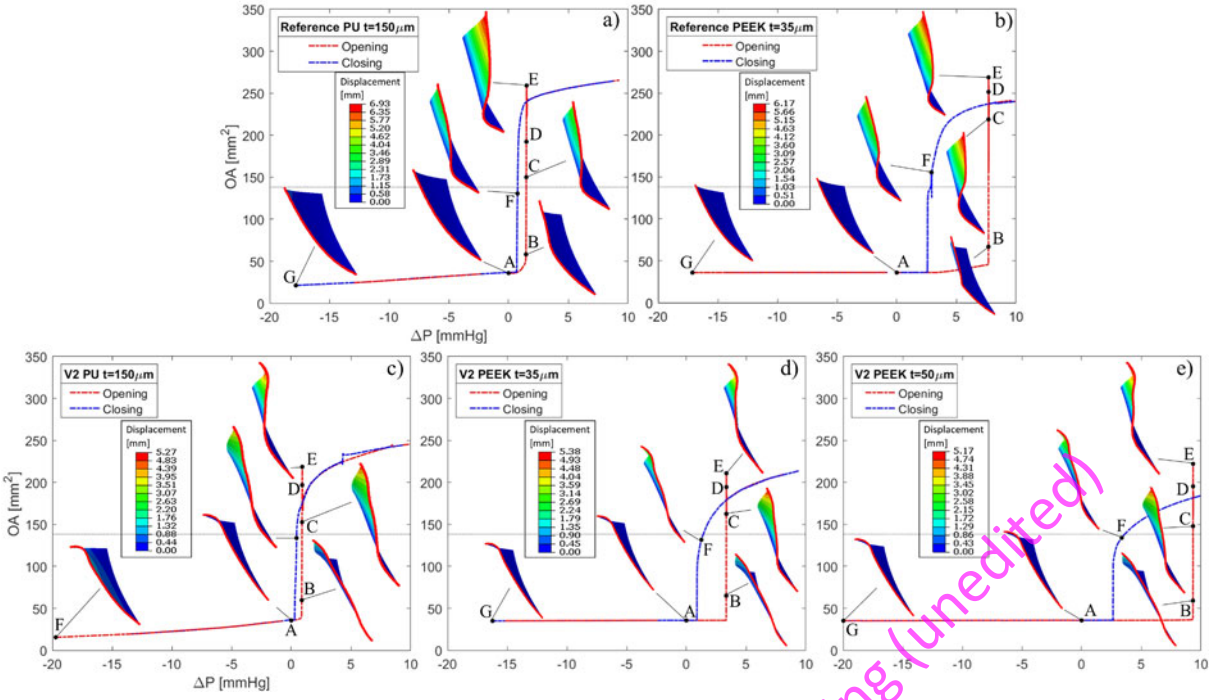


**Fig. 7: Simulated OA for one cycle (systole-diastole) over $\Delta P$ for reference valve a) PU $t$ = 150 µm, b) PEEK $t$ = 35 µm, and V2 c) PU $t$ = 150 µm, d) PEEK $t$ = 35 µm, and d) PEEK $t$ = 50 µm. Dotted line is standard value for OA for a valve that size [13]. Section views of key states (see also Fig. 8) are also illustrated, with B-C marked in red, and displacements' magnitude in mm. SM reports data from other variants.**

Preprint of Bio-Design and Manufacturing (unedited)

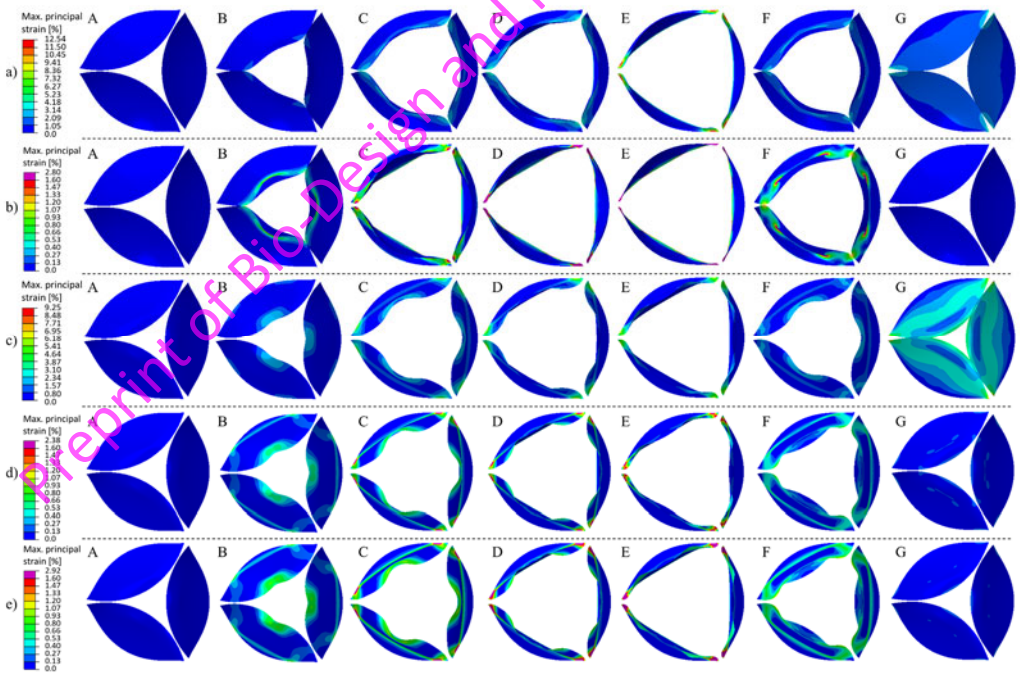


**Fig. 8 Top view of opening and closing with max. principal strain for the instants found in Fig. 7: a): reference valve (PU $t$ = 150 µm); b): reference valve (PEEK $t$ = 35 µm); c): V2 (PU $t$ = 150 µm); d): V2 (PEEK $t$ = 35 µm); e): V2 (PEEK $t$ = 50 µm); For PEEK, elements exceeding a conservative yield limit of 1.6% [51], are illustrated in purple.**

This latter phenomenon is intensified for $t$ = 50 µm, which exhibits a greater disparity in opening and closing paths. Note that, complete closing of the valve is not modeled (i.e., higher

negative pressures) as tight closing is weakly affected by the design variation, as shown by the experiments (see section 4.2), given the alike stress-free OA.

At the same instant, PU underwent a maximum logarithmic strain, $\varepsilon_{max}$, of ~12%, way below the tensile strain at break i.e., 450%. In contrast, PEEK experienced a lower $\varepsilon_{max}$ of ~3.5%. The latter is exceeding the elastic limit, expected in range of 1.8 – 3 % [9], but as illustrated in Fig. 8, $\varepsilon_{max}$ is concentrated along the stent edge towards the stent tips, relating to the fixed boundary conditions. Introducing a valve frame with a certain flexibility may not alter the location of $\varepsilon_{max}$, however, the value is expected to decrease.

#### *4.1.3 Bending and membrane states*

Fig. 9 shows the bending and membrane stresses ($\sigma_{22}$ & $\sigma_{33}$) along the normalized length (ranging from the free edge -0-, to the fixed boundary -1-) of leaflet's B-C, for the opening and maximum pressure (defined as in Fig. 3c), including both V2 in PU ($t$ = 150 μm) and PEEK ($t$ = 50 μm). The stress comparison revealed significant difference in magnitude, with PEEK ($\sigma_{max} \approx 8.0\ MPa, \varepsilon_{max} \approx 0.33\%$) exhibiting higher stress levels than PU ($\sigma_{max} \approx 0.19\ MPa, \varepsilon_{max} \approx 1.4\%$) at maximum pressure, relating to material moduli and load case, with the maximum stresses to lie in direction 2.

The calculated strain energy ratio ($\psi$) between bending and total strain energy (including both $\sigma_{22}$ & $\sigma_{33}$, Fig. 9e, f, k, l), was 0.82 and 0.87 at the opening, and 0.72 and 0.85 at maximum pressure for PU and PEEK, respectively. This suggests a bending-dominated problem in both cases, but more pronounced in PEEK, attributed to its higher stiffness. Moreover, bending stresses in direction 3, but also strain energy, are higher (especially) for PEEK, than those in direction 2, demonstrating the importance of the B-C's shape. Indicatively, the ratios of bending strain energy in direction 3, over total, at the opened state shown, are 0.55 and 0.71 for PU and PEEK, respectively.

Preprint of Bio-Design and Manufacturing (unedited)

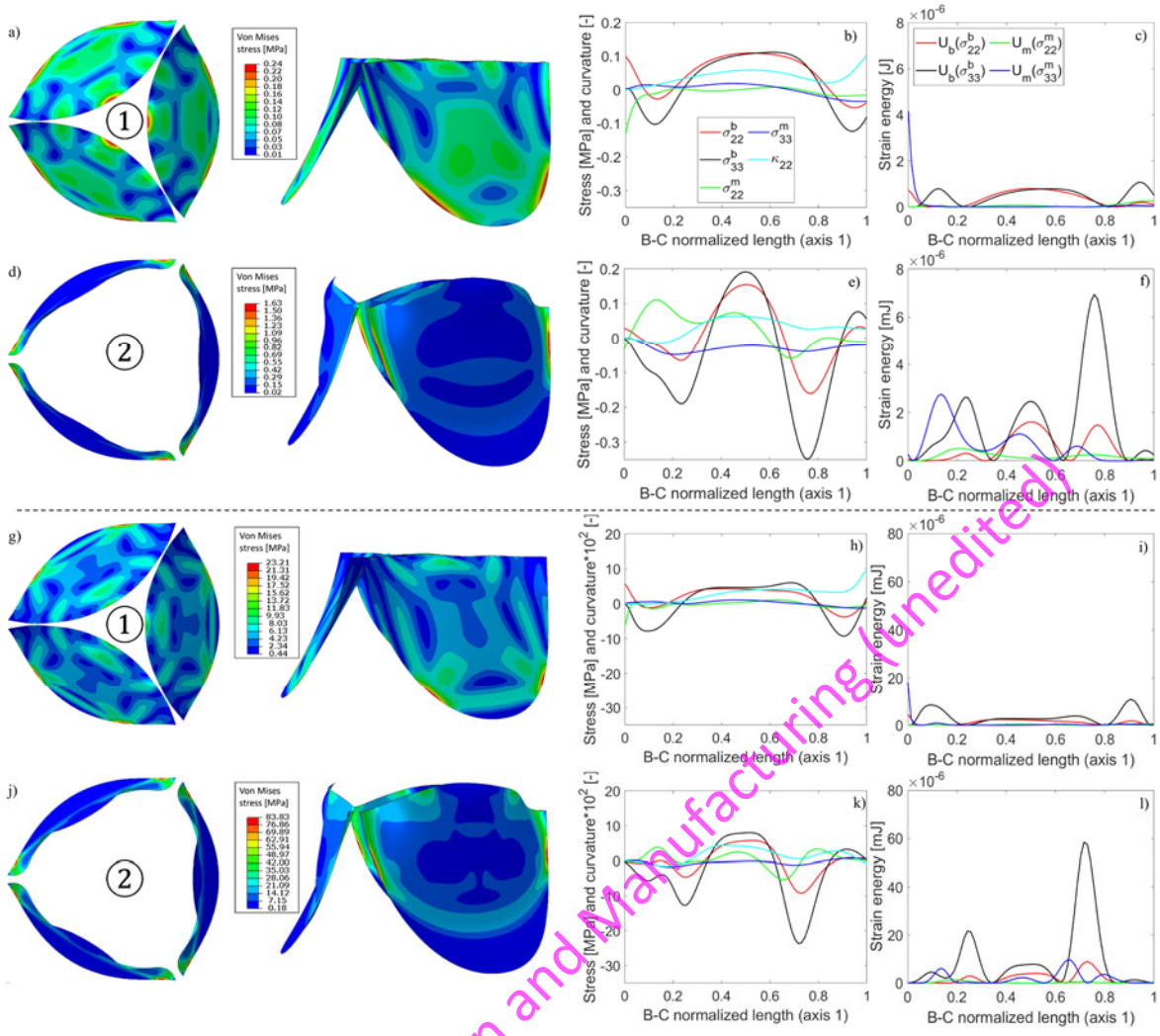


**Fig. 9: Deformed state information of V2 at opening instant ① (see Fig. 3c) and maximum pressure defined at instant ② (see Fig. 3c, ~17 mmHg). for Top: PU - $t = 150$ µm vs. Bottom: PEEK - $t = 50$ µm. From left to right: *i)* Deformed states with von Mises stresses of V2: a), d), g) & j). *ii)* Bending (at t/2 in Fig. 3) and membrane stresses around direction 2 & 3, and curvature $\kappa_{22}$: b), e), h) & k). *iii)* Bending and membrane strain energy around direction 2 & 3: c), f), i) & l). Note the scale changes.**

Preprint of Bio-Design and Manufacturing (unedited)

### 4.2 Experimental analysis

The experimental results, summarized in Fig. 10, depict similar trends to the FE simulations in OPs, for both PU and PEEK valves. The OPs for PEEK leaflets were lower than the simulation predictions (Fig. 10b), and this is mainly due to their final thickness (after thermoforming) that was in the range of 45 ± 7 µm [51], compared to simulated nominal 50 µm. Remarkably, the reference valve exhibits the highest OP (14.2 mmHg), while V2 demonstrates the lowest (8.0 mmHg), representing a 44% improvement. The $\Delta\bar{P}$s (refer also to Fig. 11e) were found to be in a physiologic range of 5.5 – 6.9 mmHg [61], and compare well with state-of-the-art BHV referencing (5 – 11 mmHg [49]). Yet, there is still potential for studies in improving the responsiveness, as discussed in section 4.3, given that BHV and MHV may demonstrate OPs as

low as ~1 and ~2 mmHg, respectively (see SM and [8]).

Despite the trend coincidence, the OPs for the PU valve are rather high compared to expectations as explained in SM (Appendix C), yet it should be noted that the tested PU valves inherited some manufacturing imperfections in thickness, attributed to the dip-coating process (also in SM). Thus, they are also compared to simulation predictions with incorporation of the measured thickness distribution from produced coupons; actual mean thickness, $\bar{t}_{exp}$, along B-C is ~250 μm.

The latter simulations are in good coincidence with the experiments, while the lower thickness (PU, $t = 150$ μm) models can relate better to literature resources [35], with a perfect coincidence when the exact material properties are employed (6 vs. 13.2 MPa, see also SM, Appendix A). Among the experimentally tested PU variants, the reference valve exhibited the highest OP (25 mmHg), while V2 showed the best OP (16.8 mmHg) with an improvement of 33%. V5 did not follow the predicted trend being the worst PU variant, suggesting that manufacturing imperfections may be of greater influence on this particular design. $\Delta\bar{P}$s (7.9 – 9.6 mmHg, see also Fig. 11e) fell within a normal to slightly elevated range. [60]

The OAs for the PU variants exceeded the values predicted by the simulations utilizing the measured thickness distribution, whereas for PEEK were lower. In most cases, the OA for PU leaflets was even less than for PEEK, but this is mainly attributed to the resulted higher thickness (and distribution) compared to literature [35] (see also SM). The OAs remained in a satisfactory range, surpassing for most cases the required value (dotted line in Fig. 10) of ~138 $mm^2$ for a valve of that diameter (i.e. 22 mm), as defined by the norm. [13] This discrepancy can be attributed to a slightly deviating geometry and fluid structure interactions, such as non-uniform pressure distributions.

Preprint of Bio-Design and Manufacturing (unedited)

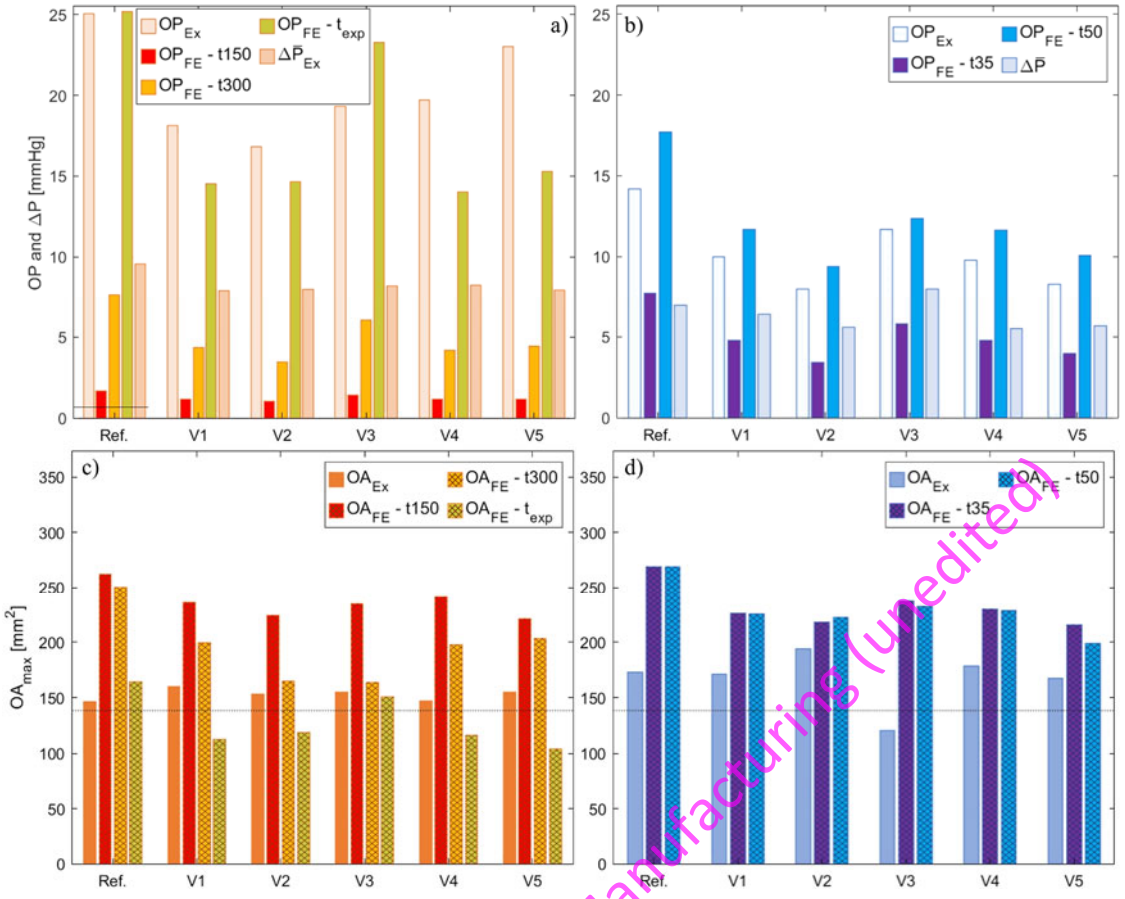


**Fig. 10: Comparison of experiments with PD and FE simulations: Top: OP and $\Delta\bar{P}$ of all designs: a) PU b) PEEK. Bottom: Maximum OA: c) PU and d) PEEK. Line in a) is OP of reference valve with E= 6 MPa, $t = 150$ µm (see SM). Dotted line in c) and d) is standard value for OA for a valve that size [13].**
**Notes: i) PU: for experiments nominal $t = 250$ µm with variation explained in SM; for simulations $t$ was fitted exponential thickness distribution, as described in SM. ii) PEEK: for experiments $t = 45 \pm 7$ µm [51], and simulations $t = 35$ µm & $t = 50$ µm.**

Preprint of Bio-Design and Manufacturing (unedited)

According to Fig. 11a, the OA of PU and PEEK leaflets for the reference valve in the PD, have some similarities over a normalized cycle, and interestingly lie in between the BHV and MHV. Yet, there were a few differences between the materials as well. The start of the opening for PEEK leaflets occurred at a very similar instant to the PU ones ($T_2$). However, the pressure build-up, and consequently OP, was significantly lower for PEEK (Fig. 11e), which align closely with the BHV. The MHV exhibited even lower OP, with an OA ~1.5× larger than that of the BHV. This is attributed to the inherent design of MHVs (bileaflet, hinged) and potentially its slightly larger inner diameter. At a fully opened state, $T_3$, the maximum OA of PEEK is greater than that of PU (see also Fig. 10c, d). Both valves exhibited tight closing behavior, although the PEEK leaflets closed faster. BHV's closing is more abrupt, yet the fully closed state happens at the same instant as the PEEK valve. The MHV also had an abrupt closing, however, delayed, a common characteristic for that valve type [8]. The PEEK leaflets appeared to have a small twist at full

closing ($T_5$), attributed to combined action of tip bending and minor inaccuracies. The PU ones, having high extensibility (much lower modulus) can show tight closing without the minor twist. The recording of the opening and closing can be found in supplementary video.

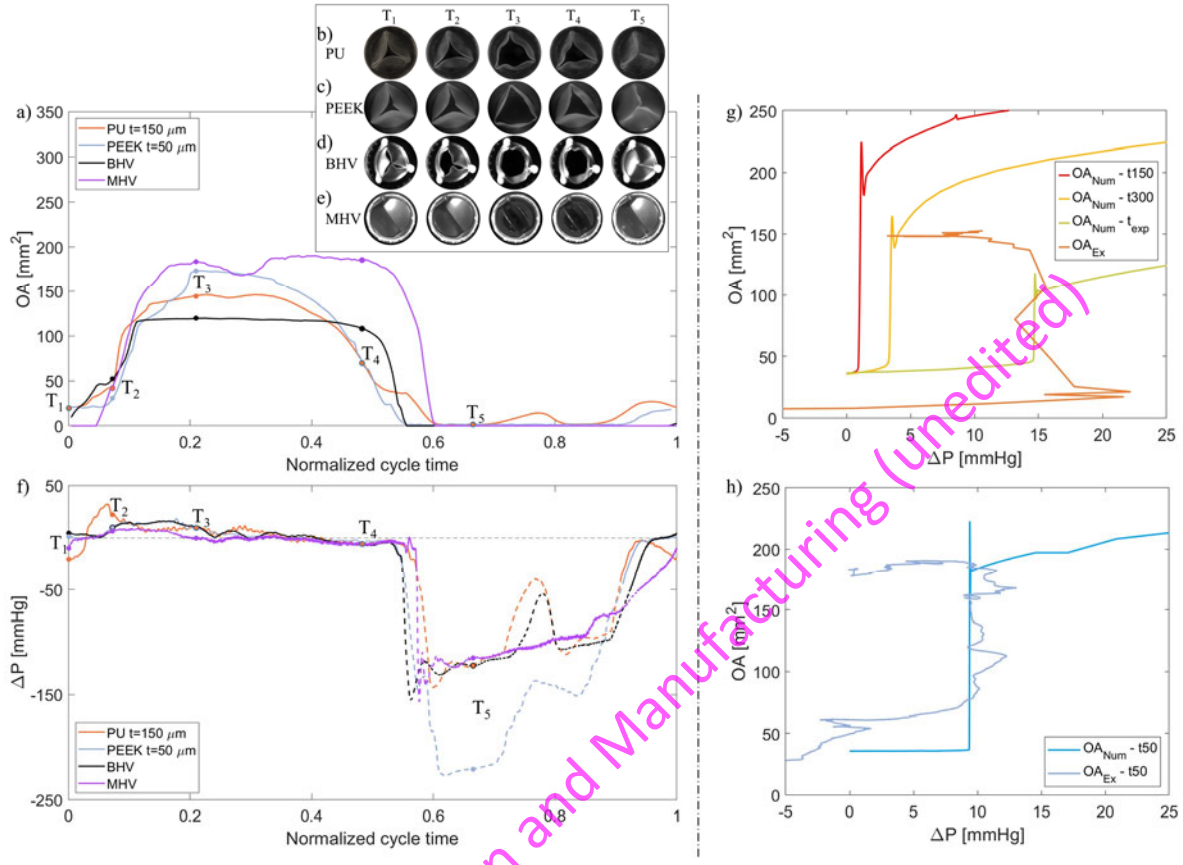


**Fig. 11: Left: a) OA plotted over normalized cycle time with key, top-view snapshots of b) reference PU ($t$ = 150 µm), c) reference PEEK ($t$ = 50 µm), d) BHV & e) MHV and f) $\Delta P$ plotted over normalized cycle time. Dashed lines contain non-indicative data out of the sensing range.**
**Right: OA plotted over $\Delta P$ (numerical and experimental) for V2 g) PU ($t$ =150 µm) and h) PEEK ($t$ = 50 µm).**

Preprint of Bio-Design and Manufacturing (unedited)

### 4.3 Discussion on shape optimality

Having identified the effect of curve radius on the buckling force (see section 3.1.2) a simulation was conducted on V2 with an increased $R_1$ of 80 mm (Fig. 2j). Despite the previously established trend of increased radius for a lower OP (see section 3.1.2), the measured OP increased by 11% compared to V2, at a value of 10.4 mmHg. This might be attributed to the flattening of B-C as the radius increases, causing the leaflet shape to approach the flat panel form, discussed in section 3.1.2.

This study explored a buckling inspired shape revealing that such shapes facilitate snap-through behavior, demonstrating potential for further investigation. Sensitivity analysis including automatized optimization may be the topic of further studies aiming to explore optimality of

adopted shape in correlation with the imposed boundary conditions. The benefit is expected to be translated on different valve sizes, but valve size shall be included in any optimization, assuming potential dependency to trigger buckled shape.

## 5. Conclusions

Having identified the lack of an idealized firm equivalent to biological leaflet for heart valve prosthesis, this study focused on the feasibility of the implementation of high-grade polymers as viable solutions for artificial heart valve leaflet-designs. This work demonstrated that materials with E-moduli, far exceeding that of biological tissues, have high potential to be used for valve leaflets, provided that designs deviate from the biomimetic ones. It becomes apparent that the leaflet behavior undergoes a transition from a mixed membrane-bending load state, to a rather bending-dominated one, as we transition from tissue-like materials (low modulus) to high-grade polymer materials (~300× higher modulus). The bending dominance, gave ground to the implementation of a double-curvature leaflet design (on B-C basis), inspired by the observed buckling modes of state-of-the-art leaflets, which extends the design space, while resulting in a substantial improvement on the opening behavior of tri-leaflet valves, with particular benefit for stiffer leaflet materials. The best performing variant shows an improvement in OP of 47% based on numerical analysis with the trends verified by the experimental in-vitro hemodynamic assay, namely 44%. This improvement places the proposed solution in a direct comparison with state-of-the-art BHV prosthesis, when comparing the achieved $\Delta\bar{P}$ of 5.6 mmHg vs. 9 mmHg. [49]

Based on the aforementioned information, we can clearly identify and propose for first time, a very promising leaflet design that can accommodate kinematics that resemble physiologic leaflet behavior using PEEK, a material with proven hemocompatibility that includes high inertness, while being one of the most mechanically performing structural polymer. Future studies should attest the combination of material-blood interaction and offered hemodynamics, to access any shear stress related blood reaction in an in vivo environment.

The most promising design may still be subject to higher level optimization, which can be founded on the adopted lean simulation scheme, having proven efficacy and reliability for performance assessment, based on the trends identified by conducted experiments.

Preprint of Bio-Design and Manufacturing (unedited)

## Author contributions

Conceptualization, Caroline C. Smid, Georgios A. Pappas, Nikola Cesarovic, Volkmar Falk, and Paolo Ermanni; Data curation, Caroline C. Smid; Formal Analysis, Caroline C. Smid and Georgios A. Pappas; Funding acquisition, Volkmar Falk and Paolo Ermanni; Investigation, Caroline C. Smid and Georgios A. Pappas; Methodology, Caroline C. Smid, Georgios A. Pappas, Nikola Cesarovic, and Paolo Ermanni; Project administration, Georgios A. Pappas; Software, Caroline C. Smid and Georgios A. Pappas; Supervision, Georgios A. Pappas and Paolo Ermanni; Validation, Caroline C. Smid, Visualization, Caroline C. Smid and Georgios A. Pappas; Writing – original draft, Caroline C. Smid and Georgios A. Pappas; Writing – review & editing, Georgios A. Pappas, Volkmar Falk, and Paolo Ermanni.

## Acknowledgements

This work was partially funded by the ETHeart initiative from the Open ETH program by the Executive Board of ETH Zurich and the Zurich Heart project of Hochschulmedizin Zürich. The authors acknowledge the support of Paul Bonnet Salvador, Tim Rogenmoser, and Damaris Bartholet on preliminary pilot simulations and experiments.

## Compliance with ethics guidelines

Caroline C. Smid, Georgios A. Pappas, Nikola Cesarovic, Volkmar Falk, and Paolo Ermanni declare that they have no conflict of interest. This study does not contain any studies with human or animal subjects performed by any of the authors.

Preprint of Bio-Design and Manufacturing (unedited)

## References

1. Qian J, Gao Z, Hou C et al. (2019) A comprehensive review of cavitation in valves: mechanical heart valves and control valves. Bio-des Manuf 2:119–136. https://doi.org/10.1007/s42242-019-00040-z
2. Windecker S, Okuno T, Unbehaun A et al. (2022) Which patients with aortic stenosis should be referred to surgery rather than transcatheter aortic valve implantation? Eur Heart J 43:2729–2750. https://doi.org/10.1093/eurheartj/ehac105
3. Yacoub MH, Takkenberg JJM (2005) Will heart valve tissue engineering change the world? Nat Clin Pract Cardiovasc Med 2:60–61. https://doi.org/10.1038/ncpcardio0112
4. Marom G, Einav S (2020) New Insights into Valve Hemodynamics. Rambam Maimonides Med J 11. https://doi.org/10.5041/RMMJ.10400

5. Bernacca GM, O'Connor B, Williams DF et al. (2002) Hydrodynamic function of polyurethane prosthetic heart valves: influences of Young's modulus and leaflet thickness. Biomaterials 23:45–50. https://doi.org/10.1016/s0142-9612(01)00077-1
6. Serino G, Gusmini M, Audenino AL et al. (2021) Multiscale Characterization of Isotropic Pyrolytic Carbon Used for Mechanical Heart Valve Production. Processes 9:338. https://doi.org/10.3390/pr9020338
7. Balguid A, Rubbens MP, Mol A et al. (2007) The role of collagen cross-links in biomechanical behavior of human aortic heart valve leaflets--relevance for tissue engineering. Tissue Eng 13:1501–1511. https://doi.org/10.1089/ten.2006.0279
8. Smid CC, Pappas GA, Falk V et al. (2024) A parametric study on pulse duplicator design and valve hemodynamics. Artif Organs. https://doi.org/10.1111/aor.14757
9. Chen MJ, Pappas GA, Massella D et al. (2023) Tailoring crystallinity for hemocompatible and durable PEEK cardiovascular implants. Biomaterials Advances 146:213288. https://doi.org/10.1016/j.bioadv.2023.213288
10. Langenaeken T, Meester P de, Verbrugghe P et al. (2023) In vivo performance of a tri-leaflet mechanical heart valve prosthesis in an ovine model. Interdiscip Cardiovasc Thorac Surg 37. https://doi.org/10.1093/icvts/ivad142
11. Carrel T, Vogt PR, Obrist D et al. (2023) Evolving technology: the TRIFLO tri-leaflet mechanical valve without oral anticoagulation: a potential major innovation in valve surgery. Front Cardiovasc Med 10:1220633. https://doi.org/10.3389/fcvm.2023.1220633
12. Young ER, Martin C, Ribaudo J et al. (2024) Surface Modification of PEEKs with Cyclic Peptides to Support Endothelialization and Antithrombogenicity. Mater Today Commun 39. https://doi.org/10.1016/j.mtcomm.2024.108664
13. International Organization for Standardization (2021) Cardiovascular implants - Cardiac valve prostheses: Part 3: Heart valve substitutes implanted by transcatheter techniques(5840-3:2021)
14. Rezvova MA, Klyshnikov KY, Gritskevich AA et al. (2023) Polymeric Heart Valves Will Displace Mechanical and Tissue Heart Valves: A New Era for the Medical Devices. Int J Mol Sci 24. https://doi.org/10.3390/ijms24043963
15. Ghanbari H, Viatge H, Kidane AG et al. (2009) Polymeric heart valves: new materials, emerging hopes. Trends Biotechnol 27:359–367. https://doi.org/10.1016/j.tibtech.2009.03.002
16. Kuan YH, Dasi LP, Yoganathan A et al. (2011) Recent Advances in Polymeric Heart Valves Research. International Journal of Biomaterials Research and Engineering 1:1–17. https://doi.org/10.4018/ijbre.2011010101
17. Oveissi F, Naficy S, Lee A et al. (2020) Materials and manufacturing perspectives in engineering heart valves: a review. Mater Today Bio 5:100038. https://doi.org/10.1016/j.mtbio.2019.100038
18. Jenney C, Millson P, Grainger DW et al. (2021) Assessment of a Siloxane Poly(urethane-urea) Elastomer Designed for Implantable Heart Valve Leaflets. Adv NanoBio Res 1:2000032. https://doi.org/10.1002/anbr.202000032
19. Rahmani B, Tzamtzis S, Sheridan R et al. (2017) In Vitro Hydrodynamic Assessment of a New Transcatheter Heart Valve Concept (the TRISKELE). J Cardiovasc Transl Res 10:104–115. https://doi.org/10.1007/s12265-016-9722-0
20. Ovcharenko EA, Seifalian A, Rezvova MA et al. (2020) A New Nanocomposite Copolymer Based On Functionalised Graphene Oxide for Development of Heart Valves. Sci Rep 10:5271. https://doi.org/10.1038/s41598-020-62122-8
21. Desai A, Vafaee T, Rooney P et al. (2018) In vitro biomechanical and hydrodynamic characterisation of decellularised human pulmonary and aortic roots. J Mech Behav Biomed Mater 79:53–63. https://doi.org/10.1016/j.jmbbm.2017.09.019

Preprint of Bio-Design and Manufacturing (unedited)

22. Snyder Y, Jana S (2023) Trilayer anisotropic structure versus randomly oriented structure in heart valve leaflet tissue engineering. Bio-des Manuf 6:423–438. https://doi.org/10.1007/s42242-023-00237-3
23. Li RL, Russ J, Paschalides C et al. (2019) Mechanical considerations for polymeric heart valve development: Biomechanics, materials, design and manufacturing. Biomaterials 225:119493. https://doi.org/10.1016/j.biomaterials.2019.119493
24. Life Sciences in Scottland (2020) Aortech announce heart valve development update. https://www.lifesciencesscotland.com/news/3488
25. John Fisher (1996) Artificial Heart Valve: United States Patent(USOO55OOO16A)
26. Bernacca GM, Mackay TG, Gulbransen MJ et al. (1997) Polyurethane Heart Valve Durability: Effects of Leaflet Thickness and Material. Int J Artif Organs 20:327–331. https://doi.org/10.1177/039139889702000606
27. International Organization for Standardization (2019) Cardiovascular implants – Cardiac valve prostheses: Part 1: General requirements(5840-1:2019)
28. Burriesci G, Marincola FC, Zervides C (2010) Design of a novel polymeric heart valve. J Med Eng Technol 34:7–22. https://doi.org/10.3109/03091900903261241
29. Gaetano F de, Serrani M, Bagnoli P et al. (2015) Fluid dynamic characterization of a polymeric heart valve prototype (Poli-Valve) tested under continuous and pulsatile flow conditions. Int J Artif Organs 38:600–606. https://doi.org/10.5301/ijao.5000452
30. Stasiak JR, Serrani M, Biral E et al. (2020) Design, development, testing at ISO standards and in vivo feasibility study of a novel polymeric heart valve prosthesis. Biomater Sci 8:4467–4480. https://doi.org/10.1039/d0bm00412j
31. The Business Research Company (2021) Prosthetic Heart Valve Devices And Equipment Global Market Report 2021: COVID 19 Impact and Recovery to 2030: Report Code - TBR519E
32. Singh SK, Kachel M, Castillero E et al. (2023) Polymeric prosthetic heart valves: A review of current technologies and future directions. Front Cardiovasc Med 10:1137827. https://doi.org/10.3389/fcvm.2023.1137827
33. Vennemann B, Rösgen T, Heinisch PP et al. (2018) Leaflet Kinematics of Mechanical and Bioprosthetic Aortic Valve Prostheses. ASAIO J 64:651–661. https://doi.org/10.1097/MAT.0000000000000687
34. Carrel T, Dembitsky WP, Mol B de et al. (2020) Non-physiologic closing of bi-leaflet mechanical heart prostheses requires a new tri-leaflet valve design. Int J Cardiol 304:125–127. https://doi.org/10.1016/j.ijcard.2020.01.056
35. Leat ME, Fisher J (1994) A synthetic leaflet heart valve with improved opening characteristics. Medical Engineering & Physics 16:470–476. https://doi.org/10.1016/1350-4533(94)90071-X
36. Wheatley DJ, Bernacca GM, Tolland MM et al. (2001) Hydrodynamic Function of a Biostable Polyurethane Flexible Heart Valve after Six Months in Sheep. Int J Artif Organs 24:95–101. https://doi.org/10.1177/039139880102400207
37. Zakerzadeh R, Hsu M-C, Sacks MS (2017) Computational methods for the aortic heart valve and its replacements. Expert Rev Med Devices 14:849–866. https://doi.org/10.1080/17434440.2017.1389274
38. Pfensig S, Kaule S, Sämann M et al. (2017) Assessment of heart valve performance by finite-element design studies of polymeric leaflet-structures. Current Directions in Biomedical Engineering 3:631–634. https://doi.org/10.1515/cdbme-2017-0132
39. Abbasi M, Azadani AN (2020) A geometry optimization framework for transcatheter heart valve leaflet design. J Mech Behav Biomed Mater 102:103491. https://doi.org/10.1016/j.jmbbm.2019.103491
40. Zhu G, Ismail MB, Nakao M et al. (2019) Numerical and in-vitro experimental assessment of the performance of a novel designed expanded-polytetrafluoroethylene stentless bi-leaflet valve for aortic valve replacement. PLoS One 14:e0210780. https://doi.org/10.1371/journal.pone.0210780

Preprint of Bio-Design and Manufacturing (unedited)

41. icu & echo Parasternal Long Axis: Mitral Valve. https://icuecho.com/windows/plax.php
42. Sabir AB, Djoudi MS (1995) Shallow shell finite element for the large deflection geometrically nonlinear analysis of shells and plates. Thin-Walled Structures 21:253–267. https://doi.org/10.1016/0263-8231(94)00005-K
43. Calladine CR (1995) Understanding imperfection-sensitivity in the buckling of thin-walled shells. Thin-Walled Structures 23:215–235. https://doi.org/10.1016/0263-8231(95)00013-4
44. Aimmanee S, Tichakorn K (2018) Piezoelectrically induced snap-through buckling in a buckled beam bonded with a segmented actuator. Journal of Intelligent Material Systems and Structures 29:1862–1874. https://doi.org/10.1177/1045389X17754270
45. Mukherjee A, Ali SF, Arockiarajan A (2021) Hybrid bistable composite laminates for structural assemblies: A numerical and experimental study. Composite Structures 260:113467. https://doi.org/10.1016/j.compstruct.2020.113467
46. Lele AG (2018) An Investigative Study of the Snapthrough, Snapback and the Stiffness Properties of a Kirigami Unit Cell. Master of Science, Clemson University
47. (2014) ABAQUS/Standard User's Manual, Version 6.14. Dassault Systèmes Simulia Corp
48. VICTREX PLC APTIV® Victrex® PEEK Film Technology. https://www.professionalplastics.com/professionalplastics/content/downloads/PeekFilm.pdf
49. Johnson NP, Zelis JM, Tonino PAL et al. (2018) Pressure gradient vs. flow relationships to characterize the physiology of a severely stenotic aortic valve before and after transcatheter valve implantation. Eur Heart J 39:2646–2655. https://doi.org/10.1093/eurheartj/ehy126
50. Adam Pick (2008) "What Is An Aortic Valve Gradient?". https://www.heart-valve-surgery.com/heart-surgery-blog/2008/10/05/aortic-valve-gradient/. Accessed 19 Feb 2024
51. Chen MJ, Pappas GA, Cesarovic N et al. (2024) Manufacturing Studies of a Polymeric/Composite Heart Valve Prosthesis. Polymer Composites. https://doi.org/10.1002/pc.28532
52. Nic An Ghaill N, Little EG (2008) Determination of the mechanical properties of Bionate 80A and Bionate 75D for the stress analysis of cushion form bearings. Proc Inst Mech Eng H 222:683–694. https://doi.org/10.1243/09544119JEIM372
53. Qi HJ, Boyce MC (2005) Stress–strain behavior of thermoplastic polyurethanes. Mechanics of Materials 37:817–839. https://doi.org/10.1016/j.mechmat.2004.08.001
54. Illenberger CM, Tobie T, Stahl K (2022) Damage mechanisms and tooth flank load capacity of oil-lubricated peek gears. J of Applied Polymer Sci 139. https://doi.org/10.1002/app.52662
55. Gulbulak U, Ertas A, Baturalp TB et al. (2020) The effect of fundamental curves on geometric orifice and coaptation areas of polymeric heart valves. J Mech Behav Biomed Mater 112:104039. https://doi.org/10.1016/j.jmbbm.2020.104039
56. Nezarati RM, Eifert MB, Dempsey DK et al. (2015) Electrospun vascular grafts with improved compliance matching to native vessels. J Biomed Mater Res B Appl Biomater 103:313–323. https://doi.org/10.1002/jbm.b.33201
57. Larson K (2019) Can You Estimate Modulus From Durometer Hardness for Silicones? Yes, but only roughly … and you must choose your modulus carefully!
58. Swanson M, Clark RE (1974) Dimensions and geometric relationships of the human aortic valve as a function of pressure. Circ Res 35:871–882. https://doi.org/10.1161/01.RES.35.6.871
59. Stanová V, Zenses AS, Rieu R et al. (2017) Effect of Valve- and Patient- Related Factors on the Effective and Geometric Orifice Areas: An In Vitro Study with the CoreValve. Comput Methods Biomech Biomed Engin 20:195–196. https://doi.org/10.1080/10255842.2017.1382929
60. Thubrikar M (1990) The aortic valve. CRC Press, Boca Raton Fla.

Preprint of Bio-Design and Manufacturing (unedited)

61. Claiborne TE, Slepian MJ, Hossainy S et al. (2012) Polymeric trileaflet prosthetic heart valves: evolution and path to clinical reality. Expert Rev Med Devices 9:577–594. https://doi.org/10.1586/erd.12.51

Preprint of Bio-Design and Manufacturing (unedited)